ARTICLES

THEORY FOR AVALANCHE OF RUNAWAY ELECTRONS IN TOKAMAKS

M.N. ROSENBLUTH, S.V. PUTVINSKI
ITER Joint Work Site,
San Diego, California,
United States of America

ABSTRACT. An analysis is presented of runaway electron formation and its evolution during disruptions in large tokamaks, where avalanche phenomena play a crucial role. A simplified, but sufficiently accurate, analytical model suitable for one dimensional (1-D) transport codes is proposed. Validation of the model was done by comparison with Monte Carlo calculations.

1. INTRODUCTION

It is known from experience in operating present tokamaks that runaway electrons can be produced during plasma disruptions, as well as during operation at low plasma densities [1–4]. High energies of the runaways, which can be accelerated by loop voltages up to 100 MeV, and high localization of their loss on the first wall make runaway electrons potentially dangerous for reducing the lifetime of the plasma facing components of tokamaks. Analysis of the disruptions in large tokamaks such as ITER [5] has shown that large machines could be more susceptible to the formation of runaway electrons than the present tokamaks, because of the effect of avalanche or multiplication of runaways due to close Coulomb collisions with the electrons of the background plasma [6, 7]. Indeed, as was shown in Ref. [7], at high loop voltage the growth rate of runaway current due to avalanche is proportional to toroidal electric field, E,

$$\gamma_{\mathrm{RA}} = \frac{1}{j_{\mathrm{RA}}}\frac{\mathrm{d}j_{\mathrm{RA}}}{\mathrm{d}t} \approx \frac{eE}{2mc\ln\Lambda}$$

where m is electron mass and $\ln\Lambda$ is the Coulomb logarithm. Taking into account that the loop voltage is produced during plasma disruption by decay of the plasma current, we can estimate the total number of e-folds during avalanche as follows:

$$\gamma_{\mathrm{RA}} t \approx \frac{eEt}{2mc\ln\Lambda} \approx \frac{I_{\mathrm{p}}}{I_{\mathrm{A}}\ln\Lambda}$$

where $I_{\mathrm{A}} = mc^3/e \approx 0.02$ MA is the Alfvén current. In the present machines with plasma currents of about 1 MA the avalanche amplification of runaway electrons gives a factor $\sim e^2$ (~ 5), but in a tokamak of ITER size the amplification factor is very large, e^{50}, which makes avalanche the primary mechanism for runaway formation in the next generation of tokamaks.

Most of the previous studies of runaway electrons were devoted to analysis of Dreicer acceleration and this source of runaways (the most important source in the present experiments) is well described analytically and numerically [8, 9], including relativistic effects [10]. The avalanche effect has received less attention in the literature. In Ref. [7], the phenomenon was estimated in the non-relativistic limit and without taking into account the effect of pitch angle scattering of the electrons. As a result, the formula for the growth rate of runaway electrons derived in Ref. [7] does not have a threshold for electric field [11] and hence predicts massive runaway formations in ITER conditions (amplification factor e^{50}!) even for the normal ohmically driven discharge. On the other hand, it is known [10, 11] that at

$$E < E_{\mathrm{c}} = \frac{4\pi e^3 n_{\mathrm{e}}\ln\Lambda}{mc^2} \qquad (1)$$

which is the case for a typical tokamak discharge, runaway generation (including avalanche phenomena) is not possible.

In the present paper, we propose a simple analytical equation describing the evolution of runaway current in tokamaks that is derived from the relativistic Fokker–Planck gyrokinetic equation for runaway electrons. The simplified equation is suitable for one dimensional (1-D) transport codes in the analysis of runaway formation. The proposed formula takes into account all the essential phenomena that affect runaway formation and is, we believe, applicable over a wide range of plasma parameters. The equation was validated by comparison with a Monte Carlo code. The numerical calculations show that the analytical formula for runaway growth rate has an accuracy of better than 20% for the plasma parameters of interest. Analysis of the energy spectra of runaway electrons has confirmed the earlier predictions [7, 12] that

avalanche phenomena will reduce the average energy of runaway electrons to 10–20 MeV.

2. ANALYTICAL SOLUTION

We shall describe runaway electrons with the gyrokinetic relativistic Fokker–Planck equation averaged over a particle bounce period,

$$\frac{\partial f}{\partial t}\oint\frac{\mathrm{d}\theta/2\pi}{\sqrt{1-\lambda b(\theta)}} + \frac{eE}{mc}\left(\frac{1}{p^2}\frac{\partial}{\partial p}p^2 f - \frac{2}{p}\frac{\partial}{\partial\lambda}\lambda f\right)\oint\sigma\frac{\mathrm{d}\theta}{2\pi} = \frac{1}{\tau}\left(\frac{1}{p^2}\frac{\partial}{\partial p}\oint\frac{\mathrm{d}\theta/2\pi}{\sqrt{1-\lambda b(\theta)}}(p^2+1)f + \frac{2(Z+1)}{p^3}\sqrt{1+p^2}\frac{\partial}{\partial\lambda}\lambda\oint\frac{\sqrt{1-\lambda b(\theta)}\,\mathrm{d}\theta}{2\pi}\frac{\partial f}{\partial\lambda}\right) + \oint S\frac{\mathrm{d}\theta/2\pi}{\sqrt{1-\lambda b(\theta)}}. \quad (2)$$

Here we have introduced the following dimensionless variables and notation:

$$p = mV/m_0c, \qquad \lambda = \frac{p_\perp^2}{p^2}\frac{1}{b(\theta)}, \qquad b(\theta) = \frac{B(\theta)}{B_{\max}}$$

$$\tau = \frac{m_0^2c^3}{4\pi n_e e^4\ln\Lambda} = \frac{m_0c}{eE_c}$$

$p_\perp$ is the component of the momentum perpendicular to the magnetic field, λ is the conserved magnetic moment, Z is the effective ion charge of the background plasma, $\sigma = \pm 1$ is the sign of the parallel momentum ('plus' corresponds to the electric field direction) and θ is the poloidal angle on circular magnetic surfaces. In Eq. (2), we have neglected corrections of the order of $(r/R)^2$. In these variables, the volume element is

$$p_\perp\,\mathrm{d}p_\perp\,\mathrm{d}p_\parallel = \frac{\sigma b(\theta)}{2}\frac{p^2\,\mathrm{d}p\,\mathrm{d}\lambda}{\sqrt{1-\lambda b(\theta)}}. \quad (3)$$

Integrals over θ in Eq. (2) are taken along the particle orbit, and hence for trapped particles $\oint\sigma\,\mathrm{d}\theta = 0$.

To introduce the avalanche source of runaway electrons, S, we need to evaluate the distribution of the secondary high energy electrons knocked out of their orbits by close collisions of a primary relativistic electron with low energy electrons from the background plasma. We have used a simplified model (the leading term in the Møller scattering) for close Coulomb collisions, which gives sufficiently accurate results in our case. In the limit, $p_1 \gg 1$, when the trajectories of the primary electrons are not much deflected by collisions the source can be presented in the form

$$S = \frac{n_r\delta(\lambda-\lambda_2)\sqrt{1-\lambda b}}{\tau\ln\Lambda}\frac{1}{p^2}\frac{\partial}{\partial p}\left(\frac{1}{1-\sqrt{1+p^2}}\right). \quad (4)$$

Here and below, the subscript '1' corresponds to the primary electrons and the subscript '2' to the secondary electrons. Energy conservation

$$\sqrt{p_1^2+1}+1 = \sqrt{p_\perp^2+p_{\parallel,2}^2+1} + \sqrt{(p_1-p_{\parallel,2})^2+p_\perp^2+1} \quad (5)$$

gives the parallel component of the momentum, $p_{\parallel,2}$, of the secondary electrons as a function of p. In Eq. (5), the perpendicular and parallel directions of momentum are referred to the momentum of the primary electrons. Taking into account that the high energy primary electrons move predominantly along the magnetic field we can determine the magnetic moment of the secondary electrons,

$$\lambda_2 b = \frac{2}{\sqrt{1+p^2}+1}.$$

The simplest solution can be found when the pitch angle scattering is small and can be neglected (this corresponds to a formal solution of Eq. (2) at $Z = -1$). In this case, all passing particles with momentum above the critical one, p_m, defined by the equation

$$\frac{eE\tau}{mc} = \left(1+\frac{1}{p_m^2}\right)\oint\frac{\mathrm{d}\theta/2\pi}{\sqrt{1-\lambda b(\theta)}} \quad (6)$$

run away and hence the growth rate of runaway electrons can be found by integrating Eq. (2) over $p > p_m$. Neglecting toroidal corrections $b(\theta) \approx 1$, the integration can be carried out. At large electric field and hence small p_m,

$$\frac{\partial n_r}{\partial t} \approx \frac{n_r}{2\tau\ln\Lambda}\left(\frac{E}{E_c}-1\right). \quad (7)$$

We now proceed to solve Eq. (2) at the large Z. The major contribution of the source given by Eq. (4) is at the low energy part of the energy spectrum, $p \approx p_m$, where pitch angle scattering is essential. We also assume that the electric field is larger than the critical field E_c, i.e.

$$2(Z+1)\frac{E}{E_c} \gg \frac{E}{E_c} \gg 1. \quad (8)$$

In this case, we can write to the lowest order,

$$\frac{\partial f_0}{\partial \lambda} = 0.$$

To the first order

$$\frac{\partial f_1}{\partial \lambda} = \left(\oint \sigma \frac{\mathrm{d}\theta}{2\pi} \Big/ \oint \frac{\sqrt{1-\lambda b(\theta)}\,\mathrm{d}\theta}{2\pi} \right) \times \frac{p^3}{\sqrt{1+p^2}} \frac{E}{E_c} \frac{1}{2(Z+1)} \frac{\partial f_0}{\partial p}. \quad (9)$$

For banana particles

$$\oint \sigma \frac{\mathrm{d}\theta}{2\pi} = 0$$

and hence $f_1(\lambda \geq 1) = 0$.

Finally, by integrating over λ to annihilate the pitch angle dependence we have

$$\frac{(E/E_c)^2}{2(Z+1)} \frac{1}{p^2} \frac{\partial}{\partial p} \frac{p^5}{\sqrt{1+p^2}} \frac{\partial f_0}{\partial p} \times \int \left[\left(\oint \sigma \frac{\mathrm{d}\theta}{2\pi} \right)^2 \Big/ \oint \frac{\sqrt{1-\lambda b(\theta)}\,\mathrm{d}\theta}{2\pi} \right] \lambda\,\mathrm{d}\lambda + \frac{2}{p^2} \frac{\partial}{\partial p} (p^2+1) f_0 = \frac{n_r}{p^2 \ln \Lambda} \frac{\partial}{\partial p} \left(\frac{1}{\sqrt{1+p^2}-1} \right). \quad (10)$$

The integral over θ represents the familiar neoclassical function arising in neoclassical resistivity for a Lorentz gas,

$$\gamma(\epsilon) = \frac{3}{4} \int \frac{\lambda\,\mathrm{d}\lambda}{\oint \sqrt{1-\lambda b(\theta)}\,\mathrm{d}\theta/2\pi} \approx \left(1 + 1.46\sqrt{r/R} + 1.72 r/R \right)^{-1} \quad (11)$$

for large aspect ratio.

The first integral of Eq. (10) over p is trivial and yields an equation of the form

$$\frac{2\gamma(\epsilon)(E/E_c)^2}{3(Z+1)} \frac{p^5}{\sqrt{1+p^2}} \frac{\partial f_0}{\partial p} + 2(1+p^2) f_0 = \frac{n_r}{\ln \Lambda} \left(\frac{1}{\sqrt{1+p^2}-1} - C \right).$$

The integration constant C is to be determined by the condition that f_0 is regular at $p = 0$ and $f_0 \to 0$ as $p \to \infty$. With

$$\beta = \frac{2\gamma}{3(Z+1)} \left(\frac{E}{E_c} \right)^2$$

this leads to the condition

$$\int_0^\infty \mathrm{d}p \frac{\sqrt{1+p^2}}{p^5} \left[\left(\sqrt{1+p^2} - 1 \right)^2 - C \right] \times \exp\left(-\frac{2}{\beta} \int_p^\infty (1+p_1^2)^{3/2} p_1^{-5}\,\mathrm{d}p_1 \right) = 0. \quad (12)$$

For $\beta \gg 1$ or $E/E_c \gg (3(Z+1)/2\gamma)^{1/2}$ the runaway threshold is non-relativistic and one can use a small expansion of the integral to determine

$$C = (2\pi\beta)^{1/2}. \quad (13)$$

In the opposite limit, $\beta \ll 1$, the runaway threshold is relativistic, $p \gg 1$, and, hence, condition (12) gives

$$C = \frac{3\beta}{2}. \quad (14)$$

Using Eq. (9), one can express particle flux in momentum space as $p \to \infty$ in terms of C, i.e. $\Gamma = (n_r/2\tau \ln \Lambda)C$, and hence the runaway rate can be described by a convenient joining formula that fits the limits given by Eqs (13) and (14)

$$\frac{1}{n_r} \frac{\partial n_r}{\partial t} = \frac{1}{\tau \ln \Lambda} \left(\frac{\pi\beta}{2} \right)^{1/2} \left(1 + \frac{8\pi}{9\beta} \right)^{1/2}. \quad (15)$$

At very small $E/E_c - 1$ this approach fails since at the runaway threshold the electric field can accelerate only particles moving parallel to the magnetic field, $\lambda \ll 1$, and the distribution function becomes quite anisotropic. In this case, the runaway threshold is relativistic and hence all the particles of interest have $p \gg 1$. At this limit Eq. (2) becomes

$$\frac{1}{p^2} \frac{\partial}{\partial p} \left(\frac{E}{E_c} - 1 - \frac{\lambda}{2} \right) p^2 f - \frac{E}{E_c} \frac{2}{p} \frac{\partial}{\partial \lambda} \lambda f - \frac{2(Z+1)}{p^2} \frac{\partial}{\partial \lambda} \lambda \frac{\partial f}{\partial \lambda} = \frac{n_r \delta(\lambda - 2/p)}{p^4 \ln \Lambda}. \quad (16)$$

At the first approximation in the small parameter $E/E_c - 1$, Eq. (16) gives

$$f = g(p) \exp\left(-\frac{E}{E_c} \frac{p\lambda}{Z+1} \right).$$

Substituting the last expression in Eq. (16) and integrating over λ one can obtain

$$pg(p) \frac{(Z+1)^2 E_c^2}{2E^2} \left[\frac{2E}{(Z+1)E_c} \left(\frac{E}{E_c} - 1 \right) - \frac{1}{p} \right] = \frac{n_r}{\ln \Lambda} \left(C - \frac{1}{p} \right).$$

Choosing C to make $g(p)$ regular we receive

$$C = \frac{2E}{(Z+1)E_c}\left(\frac{E}{E_c} - 1\right)$$

and hence

$$\frac{1}{n_r}\frac{\partial n_r}{\partial t} = \frac{1}{\tau(Z+1)\ln\Lambda}\frac{E}{E_c}\left(\frac{E}{E_c} - 1\right). \quad (17)$$

Equations (7), (15) and (17), which describe the growth rate of the runaway electrons at different limits, can be combined in an approximate fit (non-unique) valid for $E \geq E_c$:

$$\frac{1}{j_{RA}}\frac{\partial j_{RA}}{\partial t} = \frac{1}{\tau\ln\Lambda}\sqrt{\frac{\pi\gamma}{3(Z+5)}}\left(\frac{E}{E_c} - 1\right)$$
$$\times \left(1 - \frac{E_c}{E} + \frac{4\pi(Z+1)^2}{3\gamma(Z+5)(E^2/E_c^2 + 4/\gamma^2 - 1)}\right)^{-1/2}. \quad (18)$$

In the above equation we have replaced $Z+1$ by $Z+5$ in order to match the known result of Eq. (7), which is formally valid for $Z = -1$. In the case when plasma temperature is low and not all impurity ions are fully ionized, Eq. (1) for the critical electric field can be approximately generalized to include bound electrons,

$$E_c = \frac{2\pi e^3(n_e + n_T)}{mc^2}\ln\Lambda \quad (19)$$

where n_T is the total electron density including free and bound electrons, $n_T = n_e + n_b$.

3. MONTE CARLO MODELLING

To check the accuracy of Eq. (18) we have created a numerical code for the solution of Eq. (2) by means of statistical methods (Monte Carlo). The aim of Monte Carlo calculations was not only to validate the simple model but also to study the energy spectra of runaway electrons and their time evolution after onset of the electric field.

The code solves the Langevin equations derived from Eq. (2), which describe the random trajectory of an individual test particle,

$$\delta\lambda = \dot{\lambda}\Delta t + \sqrt{3D\Delta t}\,\xi \quad (20)$$

$$\delta p = \dot{p}\Delta t \quad (21)$$

Here,

$$\dot{p} = g(\lambda)E - (1 + 1/p^2)(1 + \ln p/\ln\Lambda_0) \quad (22)$$

$$\dot{\lambda} = -\beta\left(0.5\lambda - \frac{I_2}{I_1}\right) - \frac{2\lambda}{p}g(\lambda)E \quad (23)$$

$$\beta = 2(1+Z)\frac{\sqrt{1+p^2}}{p^3}(1 + \ln p/\ln\Lambda_0)$$

$$D = 2\beta\lambda I_2/I_1$$

ξ is a random number with uniform distribution from -1 to 1, and

$$g(\lambda) = 1/I_1$$

for passing particles, parallel to E

$$g(\lambda) = 0$$

for banana particles and

$$g(\lambda) = -1/I_1$$

for passing particles, antiparallel to E. At the high aspect ratio limit, $\epsilon = r/R \ll 1$, the passing particles correspond to $0 \leq \lambda < 1$ and the banana particles to $1 \leq \lambda \leq 1/(1-2\epsilon)$. For passing particles,

$$I_1 = \frac{2}{\pi\sqrt{1-\lambda+2\epsilon\lambda}}\mathrm{K}\left(\frac{2\epsilon\lambda}{1-\lambda+2\epsilon\lambda}\right)$$

$$I_2 = \frac{2\sqrt{1-\lambda+2\epsilon\lambda}}{\pi}\mathrm{E}\left(\frac{2\epsilon\lambda}{1-\lambda+2\epsilon\lambda}\right)$$

and for banana particles,

$$I_1 = \frac{2}{\pi\sqrt{2\epsilon\lambda}}\mathrm{K}(x)$$

$$I_2 = \frac{2\sqrt{2\epsilon\lambda}}{\pi}[\mathrm{E}(x) - (1-x)\mathrm{K}(x)]$$

$$x = \frac{1-\lambda+2\epsilon\lambda}{2\epsilon\lambda}.$$

Here $\mathrm{E}(x)$ and $\mathrm{K}(x)$ are full elliptic integrals. The electric field in Eqs (22) and (23) is normalized on the critical field defined by Eq. (19) and the dimensionless time in Eqs (20) and (21) is defined as $\tilde{t} = t/\tau$.

Equations (20) to (23) are equivalent to the gyrokinetic equation with one addition, an approximation to the dependence of the Coulomb logarithm on the momentum of a high energy electron

$$\ln\Lambda = \ln\left(\frac{2^{1/4}mc^2(1+p^2)^{3/4}}{\hbar\omega_p}\right)$$

where ω_p is the plasma frequency. In practice, we set the Coulomb logarithm so that $\ln\Lambda \approx 18 + \ln p$. In spite of the fact that this dependence is very weak and does not affect the growth rate of runaways much,

it is important in the late stage of runaway formation when the electric field is close to the critical one. Avalanches were introduced into the code through the source of secondary electrons described by Eq. (4). It was also assumed that the source is uniform over a magnetic surface and hence the pitch angle variable, λ, of secondary electrons was evaluated assuming a random uniform distribution of primary electron position over poloidal angle θ.

The code deals with a constant number of test particles that were followed along random orbits during a certain time, Δt, after which the source of secondary electrons is invoked and secondary particles are added to the ensemble. To preserve the number of test particles an equal number of primary test particles (chosen randomly) is replaced by secondary particles and simultaneously the weight of each particle is increased. The time step, dt, used for calculations of the random orbit of each individual particle, $dt \ll \Delta t$, was chosen automatically to provide sufficiently small random steps in p and λ. Usually we used 5000 test particles, which was sufficient to produce the energy spectrum and 2-D distribution functions. To avoid spending of run time on low energy particles, we assumed that runaway electrons are lost as soon as they slow down to below the energy at which drag exceeds electric field acceleration for an electron moving parallel to B, since acceleration is not possible at any λ. The lost particles were replaced by secondary particles when the source was generated.

4. RESULTS OF THE CALCULATIONS

The Monte Carlo code was used for two sets of runs. In the first set, the electric field was kept constant and the growth rate of the runaway current was evaluated. We compare the normalized numerical growth rate,

$$\gamma_{\mathrm{RA}}\tau = \frac{\tau}{j_{\mathrm{RA}}}\frac{\partial j_{\mathrm{RA}}}{\partial t}$$

with the one given by Eq. (18).

Figure 1 shows the ratio of growth rates as a function of electric field for three different values of Z. It can be seen that the analytical formula works very well especially at large electric fields, where its accuracy is about 5%. It can also be seen that Eq. (18) systematically underestimates the growth rate at low field but only by about 20%. We should note that in the database presented in Fig. 1 the absolute value of the growth rate varies by more than an order of magnitude. This underestimate and the roll-down of the curves at electric fields close to the critical field is explained by a p dependence in $\ln\Lambda$, which results in about a 20% increase in the critical field in comparison with Eq. (19), which was obtained without this dependence. Indeed, if one replaces $\ln\Lambda$ by $\ln\Lambda + \ln p$ in Eq. (16) then the actual critical electric field will be as follows:

$$\frac{E}{E_c} = 1 + \frac{\ln(\ln\Lambda) + \ln[(1+Z)/2]}{\ln\Lambda}. \qquad (24)$$

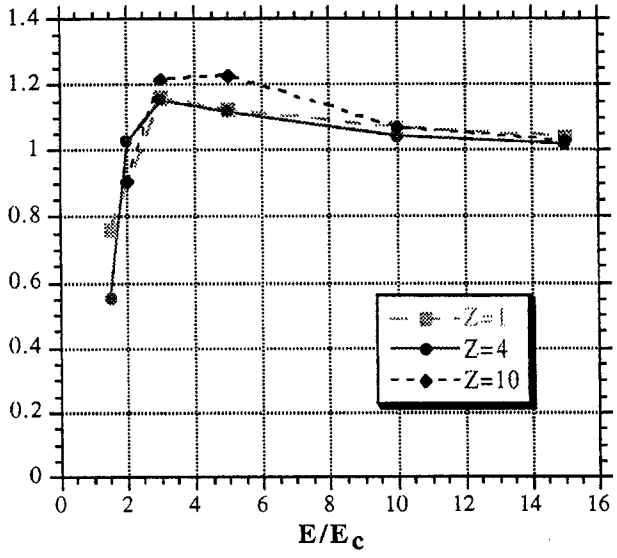

FIG. 1. Ratio of runaway growth rate calculated by the Monte Carlo code to the rate given by the theoretical formula (Eq. (18)), as a function of electric field. $\epsilon = 0.1$, $\ln\Lambda = 18$.

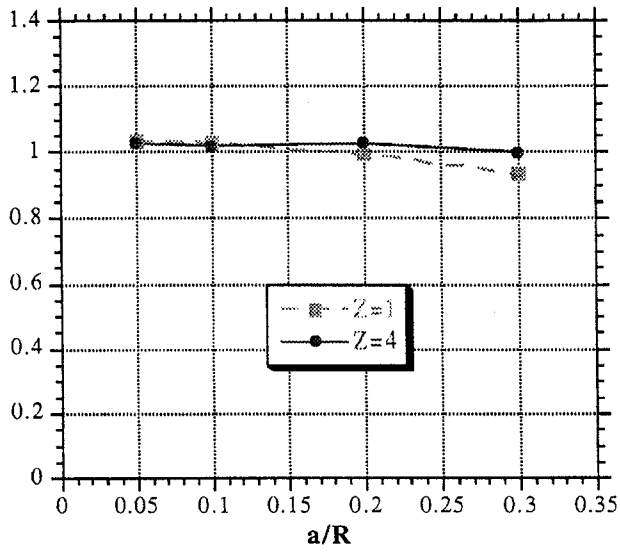

FIG. 2. Ratio of growth rate calculated by the Monte Carlo code to the rate given by the theoretical formula (Eq. (18)) as a function of inverse aspect ratio. $Z_{\mathrm{eff}} = 4$, $E/E_c = 15$, $\ln\Lambda = 18$.

Figure 2 shows the ratio of growth rates as a function of inverse aspect ratio. It can be seen that at high electric fields the analytical expression gives a good approximation to the exact solution in the wide range of plasma aspect ratio.

This conclusion was recently confirmed by the Fokker–Planck code CQL3D [13], which was used for numerical simulations of the runaway formation. The numerical results reproduce the growth rate given by Eq. (18) with an accuracy of about 10%.

The second set of runs was carried out to study the time evolution of the runaway electrons and their energy spectra. In this case, we assumed that the plasma current density, j_0, does not change and that the electric field evolves in accordance to Ohm's law,

$$E(t) = E_0 \left(1 - \frac{j_{RA}(t)}{j_0}\right) \tag{25}$$

where E_0 is the initial electric field. As in the previous case, other sources of runaway electrons were not taken into account. To start runaway buildup, we assume a small initial density of runaways all with the same initial energy and $\lambda = 0$. After a few e-folds in the growth the effect of the initial distribution dies away.

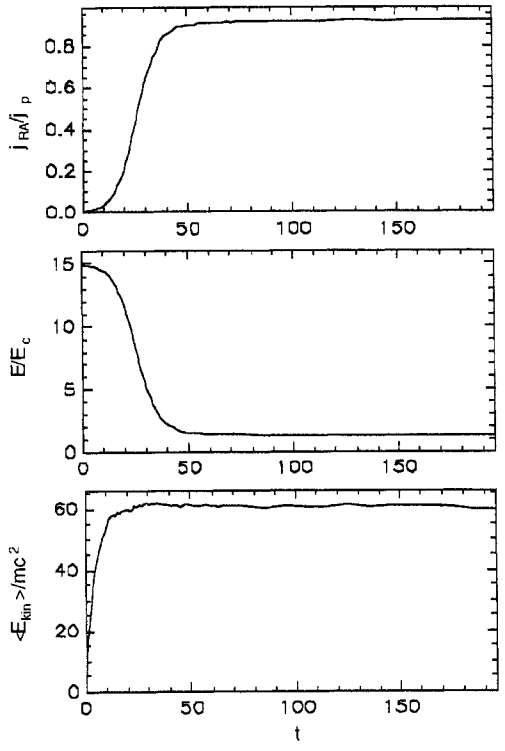

FIG. 3. Evolution of parameters during runaway electron formation. $Z_{\text{eff}} = 4$, $\ln\Lambda = 18$, $a/R = 0.1$. The time t is normalized to τ.

Figure 3 shows typical time traces of runaway current, electric field and average kinetic energy of runaway electrons. After buildup of runaway current, the electric field drops to a value slightly above the critical value described by Eq. (24). At steady state, the runaway formation by avalanche is compensated for by particles scattering out of the acceleration zone and slowing down to below p_m. Figure 4 shows the 2-D electron distribution function (only passing particles) at $t = 200$ when the global parameters have reached steady state (Fig. 3). The solid line separates the region in phase space where the particles accelerate (below the curve) and decelerate (above the curve). Pitch angle scattering, which is faster at low p, exchanges particles between these two zones. The dashed lines in Fig. 4 represent equidistant contour lines of the 2-D distribution function. Figure 5 shows the corresponding energy spectrum of the runaways obtained by integration of the 2-D distribution function over λ. It can be seen that the spectrum is close to an exponential one.

Figure 6 shows the average kinetic energy of runaways as a function of Z_{eff}. As one would expect, an increase in Z_{eff} leads to an increase in the particle scattering, a larger loss of runaways from the acceleration zone and a larger electric field at steady state. As a result, the average energy is more than twice as large in the 'dirty' plasma with $Z_{\text{eff}} = 10$

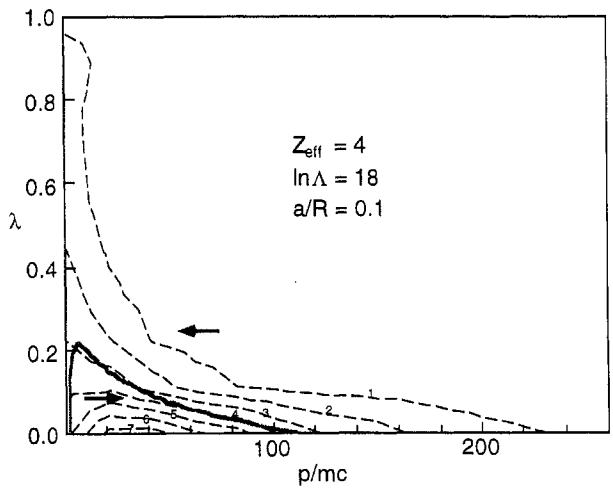

FIG. 4. Two dimensional distribution (pitch angle λ, momentum p) of transient particles at $t/\tau = 200$ in the plasma with $Z_{\text{eff}} = 4$, $\ln\Lambda = 18$ and $a/R = 0.1$. Initial electric field $E/E_c = 15$, final electric field $E/E_c = 1.23$. The solid line corresponds to an equilibrium between particle acceleration by electric field and slowing down by the drag force, i.e. $dp/dt = 0$. The arrows show the direction of particle flow in phase space.

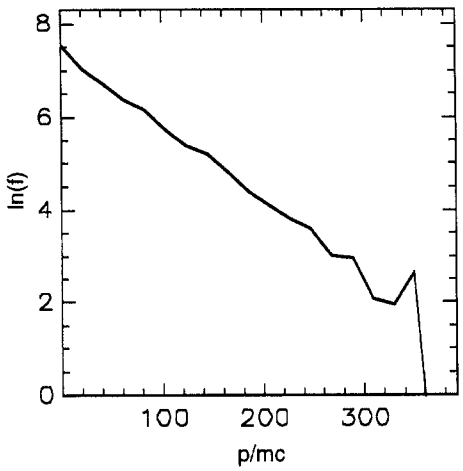

FIG. 5. Energy spectrum of runaway electrons at $t/\tau = 200$ in the plasma with $Z_{\text{eff}} = 4$, $\ln\Lambda = 18$ and $a/R = 0.1$. Initial electric field $E/E_c = 15$.

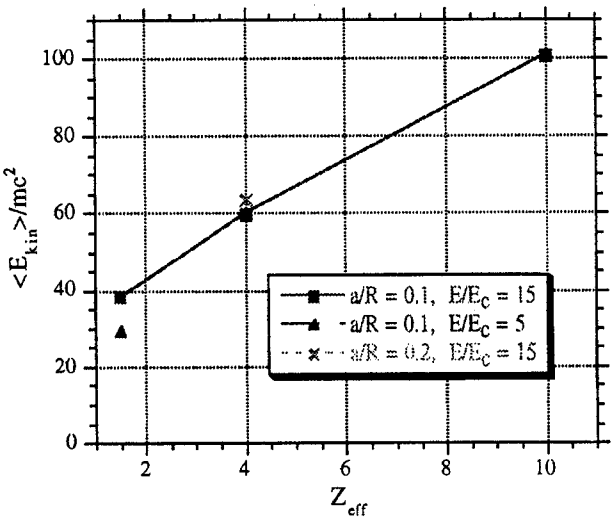

FIG. 6. Average kinetic energy of runaway electrons at $\gamma t = 50$ as a function of Z_{eff}. $\langle E_{\text{kin}}\rangle/mc^2 = \langle(p^2/m^2c^2 + 1)^{1/2} - 1\rangle$, $\ln\Lambda = 18$.

than in a hydrogen plasma with $Z = 1$. It was found that the steady state spectra are not very sensitive to the other parameters, such as aspect ratio or initial electric field. The following formula approximates the energy spectrum of runaway electrons produced by avalanche:

$$\frac{1}{n_{\text{RA}}}\frac{\mathrm{d}n_{\text{RA}}}{\mathrm{d}E} \cong \exp(-E/T) \qquad (26)$$

where

$$T\ (\text{MeV}) \cong 17.0 + 3.4Z.$$

Note that a comparison of the electron runaway rate at high E with the rate at which the tail is accelerated would predict

$$T \approx mc^2 \ln\Lambda \sqrt{\frac{3(Z+5)}{\pi\gamma}}$$

which is close to the above numerical fit, Eq. (26). At high Z (>10) the energy can be as large as 50 MeV, but in the post-disruption plasma when runaway electrons are formed one can expect a very low temperature and as a result only partially ionized impurity ions. Modelling has shown [5] that at this phase Z_{eff} is usually less than 2 and is not very sensitive to kind and amount of impurity. In addition, most electrons are bound and $\ln\Lambda$ can be as low as 10, which also reduces runaway energy. Therefore, one can expect that in the case of interest the average energy of runaway electrons will be in the range from 10 to 15 MeV.

5. CONCLUSIONS

We have found that the model for runaway formation given by the analytical expression (18) has sufficient accuracy for the description of the avalanche of runaways in tokamaks over a wide range of plasma parameters. The simplicity of the equation makes it effective for applications in 1-D transport codes. As reported elsewhere [5], such calculations show that (assuming good flux surfaces) large runaway currents are to be expected in high current tokamaks after thermal quench unless the post-disruption plasma has a very high hydrogen density, $n_{\text{DT}} \approx (3\text{–}5)\times 10^{21}$ m^{-3} and the critical field is not exceeded. The Monte Carlo calculations confirm earlier predictions [7, 12] that, under the conditions when avalanches dominate the generation of runaways, the average energy of the electrons is not very high, i.e. 10 to 15 MeV.

REFERENCES

[1] GILL, R.D., Nucl. Fusion **33** (1993) 1613.
[2] JASPERS, R., et al., Nucl. Fusion **33** (1993) 1775.
[3] JANOS, A.C., et al., in Plasma Physics and Controlled Nuclear Fusion Research 1992 (Proc. 14th Int. Conf. Würzburg, 1992), Vol. 1, IAEA, Vienna (1993) 527.
[4] KNOEPFEL, H., SPONG, D.A., Nucl. Fusion **19** (1979) 785.
[5] PUTVINSKI, S., et al., J. Nucl. Mater. **241–243** (1997) 316.
[6] SOKOLOV, Yu.A., JETP Lett. **29** (1979) 244.

[7] JAYAKUMAR, R., FLEISCHMANN, H.H., ZWEBEN, S., Phys. Lett. A **172** (1993) 447.
[8] PARAIL, V.V., POGUTSE, O.P., in Reviews of Plasma Physics, Vol. 11 (KADOMTSEV, B.B., Ed.), Consultants Bureau, New York (1986) 1.
[9] RUSSO, A.J., CAMPBELL, R.B., Nucl. Fusion **33** (1993) 1305.
[10] CONNOR, J.W., HASTIE, R.J., Nucl. Fusion **15** (1975) 415.
[11] FUSSMANN, G., Nucl. Fusion **19** (1979) 327.
[12] ROSENBLUTH, M.N., et al., in Fusion Energy 1996 (Proc. 16th Int. Conf. Montreal, 1996), Vol. 2, IAEA, Vienna (1997) 979.
[13] CHIU, S.C., et al., in Sherwood International Fusion Theory Conference (Proc. Conf. Madison, 1997), paper 2B02.

(Manuscript received 21 May 1997
Final manuscript accepted 1 August 1997)

E-mail address of S.V. Putvinski:
putvins@iterus.org

Subject classification: F3, Tt